Proc. Natl. Acad. Sci. USA
Vol. 73, No. 11, pp. 3798–3802, November 1976
Chemistry

Resonance enhanced coherent anti-Stokes Raman scattering

(Raman spectroscopy/resonance enhancement)

BRUCE HUDSON*, WILLIAM HETHERINGTON III*, STEPHEN CRAMER*, ILAN CHABAY†, AND GARY K. KLAUMINZER‡

* Department of Chemistry, Stanford University, Stanford, California 94305; † Analytical Chemistry Division, National Bureau of Standards, Washington, D.C. 20234; and ‡ Molectron Corporation, 177 N. Wolfe Road, Sunnyvale, California 94086

Communicated by James P. Collman, July 22, 1976

ABSTRACT **Resonance enhancement of coherent anti-Stokes Raman scattering due to the proximity of the laser frequencies to an electronic transition has been demonstrated for dilute solutions of diphenyloctatetraene in benzene. The Raman contribution to the third order susceptibility is shown to be complex near an electronic resonance and the resulting features of the coherent anti-Stokes Raman scattering spectra are discussed in detail. This work represents one step in the demonstration that the high signal to noise ratio, fluorescence rejection, and low average power levels of the coherent anti-Stokes Raman scattering experiment can be used to advantage in Raman studies of dilute solutions and materials of biological interest.**

Coherent anti-Stokes Raman scattering (CARS) is a nonlinear optical technique that may be used to obtain Raman spectra with a greatly enhanced signal to noise ratio and essentially complete rejection of fluorescence using average power levels which are often one or two orders of magnitude lower than used for the corresponding spontaneous Raman experiment (1–4). The work to be described here deals only with the application of CARS to the study of dilute solutions, motivated by an interest in studies of biological macromolecules. References to other applications of CARS and the basic theory are given in refs. 1–4. The most comprehensive treatment of the theory is given in refs. 5 and 6. In a CARS experiment two laser beams with frequencies ω and $\omega - \Delta$ are incident on the sample. A signal beam is generated at the frequency $\omega + \Delta$. The intensity of this signal is greatly enhanced when the frequency interval Δ is equal to a molecular vibrational frequency. Spectra are usually obtained with one frequency fixed while the other is scanned so that Δ varies through the region of the vibrational spectrum of interest. The enhanced signal to noise ratio of CARS arises from a higher conversion efficiency, the production of the signal as a collimated beam, and the fact that a large monochromator is not required. The signal to noise advantage over the spontaneous Raman effect can be ten orders of magnitude. The fluorescence rejection arises from the signal collimation and the fact that the signal is at the anti-Stokes frequency, $\omega + \Delta$.

The difficulty encountered in the application of CARS to dilute solutions is that there is a background signal at the frequency $\omega + \Delta$ due to a nonresonant electronic susceptibility. This background signal is a slowly varying function of Δ. It has the same spatial and power dependence as the vibrationally resonant signal of interest. In the absence of the electronic resonance effects to be described below, the background signal due to the solvent and the CARS signal due to the solute are equal for concentrations on the order of a few tenths molar (see Fig. 1).

The major disadvantage of a fluorescence background in a spontaneous Raman experiment is the increased shot noise which is given by the square root of the total signal. In the CARS case, however, the signal levels are on the order of 10^{10} photons per second or higher, so that even if the nonresonant background level is one hundred times larger than the CARS signal it could, in principle, be simply subtracted and still leave a signal to shot noise ratio of at least 1000:1. The important practical limitation in dilute solution studies is the noise due to laser fluctuations and beam deflections rather than the background level *per se*. An important practical difference between fluorescence and the solvent background signal of the CARS experiment is that for common solvents the background signal does not increase appreciably as the laser frequencies are moved into proximity to a solute electronic transition where electronic resonance enhancement occurs. The fluorescence signal will generally increase substantially under these conditions. This means that fluorescence often prevents full utilization of resonance enhancement in spontaneous Raman experiments.

The peak signal intensity in a CARS spectrum is proportional to the square of the power at the pump frequency ω times the power at the Stokes frequency $\omega - \Delta$. This means that it is possible to use pulsed lasers that provide high peak power, and thus high signals, but that have low average power. The experiments to be described here use only 1 or 2 mW of average power rather than typically 100 mW usually used in spontaneous Raman experiments. This reduction in average incident power should result in decreased sample damage due to those photochemical and thermal processes that are linearly dependent on the average power level.

MATERIALS AND METHODS

The CARS spectrometer used in these studies is based on a Molectron UV-1000 pulsed nitrogen laser which pumps two tunable dye lasers. The experimental arrangement is described in detail elsewhere (4). Certain features of CARS experiments that are peculiar to electronic resonance enhancement are discussed below under *Experimental Considerations*.

Diphenyloctatetraene has been the subject of previous spectroscopic study (7) including Raman spectroscopy (ref. 7, Fig. 11). This compound has a strong near UV electronic transition with maxima in benzene at 4040 Å (ϵ = 177,000 liters mole^{-1} cm^{-1}), 3810 Å (ϵ = 198,000 liters mole^{-1} cm^{-1}) and 3630 Å (ϵ = 134,000 liters mole^{-1} cm^{-1}). The oscillator strength for this transition is about 1.4. It is well-known that polyenes in general show very strong resonance enhancement of their Raman spectra (8–11). The strongest lines in the Raman spectrum of diphenyloctatetraene are at 1580, 1571, and 1140 cm^{-1} with decreasing intensity in the order given (7). The fluorescence quantum yield for diphenyloctatetraene in benzene is approximately 0.15 (12).

Absorption spectra were obtained with a Cary 14 spec-

Abbreviation: CARS, coherent anti-Stokes Raman scattering.

trometer. Spontaneous Raman spectra were recorded with a Spex Ramalog Spectrometer using a Coherent Radiation model 52 mixed gas laser and photon counting detection.

THEORETICAL CONSIDERATIONS

Certain aspects of the theory of CARS that pertain to electronic resonance enhancement have not been treated explicitly in previous publications. In particular, it will be emphasized that the CARS susceptibility, $\chi_r^{(3)}$, has resonances when ω or $\omega + \Delta$ equals an electronic transition frequency of the molecule. This result is contained in ref. 6, but the equations of ref. 5 are incorrect in this respect. Furthermore, the third order susceptibility which gives rise to the vibrational CARS signal becomes complex near an electronic resonance with potentially important consequences. In the following discussion we will ignore factors of 3 and other small numerical constants since they do not affect the argument.

The third-order susceptibility $\chi^{(3)}_{lmno}$ is defined in terms of the polarization induced in the l-direction due to the presence of fields at frequencies ω and $\omega - \Delta$.

$$P_l^{(3)}(\omega + \Delta, r) = \chi^{(3)}_{lmno} E_m(\omega, r) E_n(\omega, r) E_0^*(\omega - \Delta, r) \times \exp[i(2k_\omega - k_{\omega-\Delta})r]. \quad [1]$$

Repeated subscripts indicate summation over polarization components. The exponential factor gives rise to constructive interference for the fields produced at r in the direction $k_{\omega+\Delta} = 2k_\omega - k_{\omega-\Delta}$. This polarization oscillates at frequency $\omega + \Delta$ and gives rise to an outgoing beam whose intensity is proportional to the absolute square of $\chi^{(3)}$. This susceptibility is the sum of two terms

$$\chi^{(3)} = \chi_E^{(3)} + \chi_R^{(3)} \quad [2]$$

where we neglect the direction subscripts. $\chi_E^{(3)}$ is known as the electronic or background susceptibility. It is composed of two types of terms: those that are resonant when 2ω equals a two-photon allowed transition of the medium and other terms that do not have any two-photon (sum or difference) resonances. $\chi_R^{(3)}$ is known as the Raman susceptibility because it is resonant when Δ is equal to a Raman active vibrational interval for the medium (5), i.e.,

$$\chi_R^{(3)} = \sum_r \chi_r^{(3)} / [\omega_r - \Delta - i\Gamma_r] \quad [3]$$

where ω_r and Γ_r are the Raman vibrational frequency and linewidth, respectively. This expression must be summed over all Raman resonances, but when $\Delta \approx \omega_r$ one term will dominate. The point is that $\chi_E^{(3)}$ is a slowly varying function of Δ and is much smaller than the value of $\chi_R^{(3)}$ near $\Delta = \omega_r$. For benzene, the ratio of the real to the imaginary part of $\chi_E^{(3)}$ is greater than 100 for $\lambda_1 = 5450$ Å (13), so this quantity may be considered to be real. The factor $\chi_r^{(3)}$ which appears in Eq. [3] contains the same electric dipole transition moments and energy denominators as appear in the expression for the Raman cross section. When $\Delta = \omega_r$, $\chi_r^{(3)}$ is related to the Stokes Raman cross section by the proportionalities

$$\chi_r^{(3)} \propto \alpha^*(\omega)\alpha(\omega + \Delta) \quad [4]$$

and

$$(d\sigma/d\Omega)_\omega \propto |\alpha(\omega)|^2 \quad [5]$$

where $(d\sigma/d\Omega)_\omega$ is the Stokes Raman cross section per molecule for incident frequency ω integrated over final frequency. $\chi_R^{(3)}$ becomes large whenever ω or $\omega + \Delta$ equals (or nearly equals) a transition frequency for an electric dipole allowed transition. Far from these one-photon resonances $\alpha(\omega) \approx \alpha(\omega + \Delta)$ so $\alpha^*(\omega)\alpha(\omega + \Delta) \approx |\alpha(\omega)|^2$ and the susceptibility $\chi_R^{(3)}$ at $\Delta = \omega_r$ is pure imaginary (see Eq. [3]). In this case the absolute square of the total $\chi^{(3)}$ contains three terms: the first is the absolute square of the background susceptibility, the second is a Lorentzian of width Γ_r centered at $\Delta = \omega_r$ with a peak value given by the square of Eq. [4], the third is a "dispersive" cross term which is zero at $\Delta = \omega_r$, positive for $\Delta < \omega_r$, and negative for $\Delta > \omega_r$ and whose magnitude depends on the product of $\chi_E^{(3)}$ and $\chi_R^{(3)}$. For pure liquids where $|\chi_R^{(3)}| \gg |\chi_E^{(3)}|$ the CARS spectrum swept as a function of Δ looks like the square of a Raman spectrum with a flat background two orders of magnitude below the Raman peak intensity and an antiresonance for $\Delta > \omega_r$ where the signal drops by another two orders of magnitude (13, 14).

For a dilute solution the background will be dominated by the solvent, and the spectrum near the Raman resonances of the solute will be like those shown in Fig. 1, where the nonresonant background level is comparable to the Raman resonance signal and the negative antiresonances are easily seen on the high frequency side of each resonance.

Near an electronic resonance the α's of Eq. [4] have significant imaginary components resulting in a complex Raman susceptibility even when $\Delta = \omega_r$. When ω or $\omega + \Delta$ is close to an electronic resonance, the spectrum changes shape rapidly as ω is varied. In particular, the cross term between $\chi_E^{(3)}$ and $\chi_R^{(3)}$ is no longer zero for $\Delta = \omega_r$ and can be large and negative for dilute solutions so that a minimum occurs at the Raman resonance.

The complex nature of $\chi_r^{(3)}$ near an electronic resonance is an important consideration in the interpretation of resonance enhanced CARS spectra and in the choice of optimum experimental parameters for obtaining a spectrum. Since this point has not been made elsewhere it will be discussed in more detail. A simplified notation will be used where the background term $\chi_E^{(3)}$ is designated by B, $\chi_r^{(3)}$ is broken into its real and imaginary parts R and I, and $\delta = \omega_r - \Delta$ is the degree of detuning of the frequency difference and the Raman resonance. A spectral scan consists of changing δ from negative to positive values. The signal intensity at the frequency $\omega + \Delta$ is proportional to the absolute square of the total $\chi^{(3)}$ and in this notation is

$$|\chi^{(3)}|^2 = B^2 + (R^2 + I^2)/(\delta^2 + \Gamma_r^2) + 2BR\delta/(\delta^2 + \Gamma_r^2) - 2BI\Gamma_r/(\delta^2 + \Gamma_r^2). \quad [6]$$

The background susceptibility B has been assumed to be real. The quantities R and I are functions of δ near the electronic resonance, but for purposes of illustration will be assumed to be constant for small variations of δ. The first term on the right-hand side of Eq. [6] is the (solvent) background signal, the second is the CARS resonance, which is maximal at $\delta = 0$, and the third term is the dispersion shaped cross term which gives rise to negative dips for $\delta < 0$ ($\Delta > \omega_r$) as in Fig. 1. [The fact that the third term is negative for $\delta < 0$ contains the information that BR is positive (13).] The last term is essentially zero away from an electronic resonance where $I \approx 0$. It has the same resonance behavior as the second term and, in contrast to the third term, has the same sign for all δ. Furthermore, as the solution is diluted, the second term decreases as the number density squared while the last term decreases essentially linearly as the number density and will become the dominant term for sufficiently dilute solutions.

If $|I| \gg |R|$, the second term becomes proportional to I^2 and the third term is negligible for δ near zero. Furthermore, the

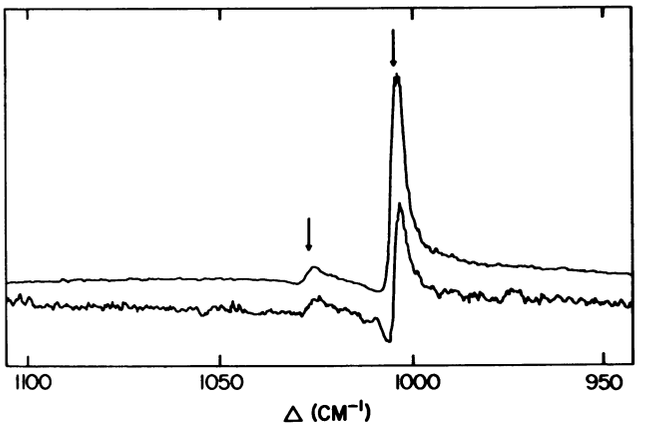

FIG. 1. CARS spectra of aqueous solutions of sodium benzoate. The upper trace is for a 1 M solution, and the full scale signal is 2.5 V. The spectrum has been shifted up slightly for clarity. The lower trace is for a 0.3 M solution, and the full scale signal is 0.7 V. The true zero level is shown in this case to indicate the background signal level for water. The arrows indicate observed Raman resonances at 1005 cm^{-1} and 1027 cm^{-1} for sodium benzoate in aqueous solution.

sign of I is positive so that the contribution of the fourth term is negative. If $I^2 + R^2 - 2BI\Gamma_r < 0$, the resonance observed at $\delta = 0$ is negative so that the total intensity is below the background level. Since the third term of Eq. [6] is negligible under these circumstances, the resonance will be below the background for all δ and there will be a minimum at $\delta = 0$. Contributions from the third term or variations of R and I with δ may shift the resonance minimum slightly from $\delta = 0$. The situation where $R^2 + I^2 - 2BI\Gamma_r = 0$ is to be avoided, since in this case there may be no appreciable CARS resonance at $\Delta = \omega_r$.

In order to illustrate the complex nature of $\chi_r^{(3)}$ near an electronic resonance, we give the explicit form for this susceptibility (6). In our notation

$$\chi_r^{(3)} = R + iI = \left(\frac{NL}{4\hbar}\right)\left(\frac{e^2}{\hbar}\right)^2 \times \sum_b \left(\frac{\langle g|X|b\rangle\langle b|X|r\rangle}{\omega_b - (\omega + \Delta) - i\Gamma_b} + \frac{\langle g|X|b\rangle\langle b|X|r\rangle}{\omega_b + \omega - i\Gamma_b}\right) \times \sum_a \left(\frac{\langle g|X|a\rangle\langle a|X|r\rangle}{\omega_a - \omega - i\Gamma_a} + \frac{\langle g|X|a\rangle\langle a|X|r\rangle}{\omega_a + (\omega - \Delta) - i\Gamma_a}\right)^*. \quad [7]$$

Polarization subscripts have been omitted from the matrix elements of the electronic position operator X. L is a local field correction, a and b label the excited electronic states, and N is the number density. For the case where only one excited electronic state is important because of the frequencies or the electric dipole matrix elements, or both, we have

$$R + iI \approx NK\{[\omega_e - (\omega + \Delta) - i\Gamma_e][\omega_e - \omega + i\Gamma_e]\}^{-1} \quad [8]$$

with

$$K = \left(\frac{Le^4}{4\hbar^3}\right)|\langle g|X|e\rangle|^2|\langle r|X|e\rangle|^2. \quad [9]$$

From Eq. [8] it is easy to show that for this isolated electronic resonance case,

$$I = U/(U^2 + V^2); R = V/(U^2 + V^2) \quad [10]$$

where $U \equiv \Gamma_e\Delta$, $V \equiv D(D - \Delta) + \Gamma_e{}^2$, and $D \equiv \omega_e - \omega$. The imaginary part, I, is always positive for this case. Away from the resonance at ω_e (large $|D|$), the imaginary component is negligible as expected. For $D = 0$ or $D - \Delta = 0$ the ratio $I/R = \Delta/\Gamma_e$, which may be large. Since I is always positive, the

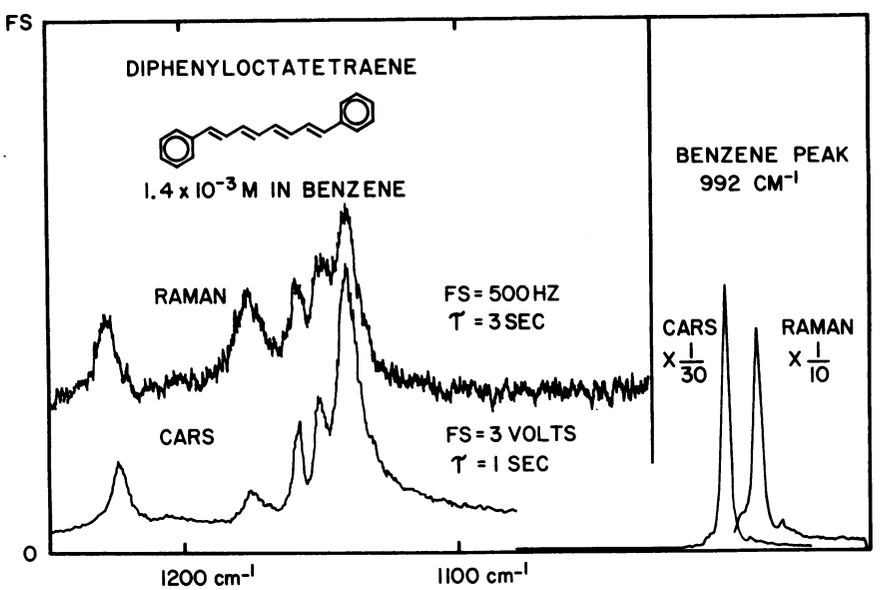

FIG. 2. CARS and spontaneous Raman spectra of a solution of diphenyloctatetraene in benzene. The concentration is 1.4×10^{-3} M (mole ratio, 1.2×10^{-4}). The Raman spectrum is on a wave-number scale, while the CARS spectrum is on a wave-length scale. The spectra are aligned at the 1140 cm^{-1} peak of diphenyloctatetraene. The slits of a Spex double monochromator were set for 1 cm^{-1} bandwidth for the Raman spectrum. The dye laser bandwidth for the CARS spectrum was 0.3 cm^{-1}. The pump wavelength for the CARS spectrum was 4800 Å, while the excitation wavelength for the Raman spectrum was 4880 Å. Full scale (FS) for the Raman spectrum represents about 5×10^3 photons sec^{-1}. For the CARS spectrum full scale is 3 V from a photodiode which corresponds to about 5×10^{10} photons per sec. The signal zero level is the same for both spectra. The background level is due to fluorescence for the spontaneous Raman spectrum. The nonresonant susceptibility produces the background in the CARS spectrum. The spectral peaks from right to left are at 992, 1140, 1150, 1157, 1175, and 1228 cm^{-1}. The peak at 992 cm^{-1} is due to benzene. Most of the intensity of the peak at 1175 cm^{-1} is also due to a benzene vibration (7).

fourth term in Eq. [6] is always negative. For two values of D the quantity V (and thus R) becomes zero. Between these two values R is negative, which will invert the sign of the third term of Eq. [6]. The complex nature of $\chi_r^{(3)}$ must be considered near an electronic resonance and all four terms of Eq. [6] must be retained.

EXPERIMENTAL CONSIDERATIONS

There will normally be some absorption of the incoming and outgoing beams under conditions of resonance enhancement. This leads to an optimum crossing position in the sample cell, an optimum concentration for given excitation, and signal frequencies, and an optimum frequency ω. The effective interaction length for the two crossed beams is on the order of a millimeter for the usual focusing conditions. If the sample cell is longer than this interaction length, then the optimum crossing position is determined by the sign of the extinction coefficient difference $2\epsilon(\omega) + \epsilon(\omega - \Delta) - \epsilon(\omega + \Delta)$. If this quantity is positive, the optimum position is at the front cell surface; if it is negative, it is at the exit surface.

For a given position of the crossing point in the cell there may be an optimum concentration due to the competition of absorption with signal generation. If the optimum is considered to be the situation that maximizes the peak signal relative to the background, then there is no optimum concentration since the background is attenuated by absorption to the same extent as the Raman peak signal. However, in practice, it is desirable to maximize the signal at $\delta = 0$. For dilute solutions the optimum concentration is given by

$$c_{opt} = [(\gamma + 2c_0) + (\gamma^2 + 4c_0^2)^{1/2}]/2 \quad [11]$$

where

$$\gamma = +2\bar{I}B\Gamma_r/(\bar{R}^2 + \bar{I}^2) \quad [12]$$

and

$$1/c_0 = 2.303\{[2\epsilon(\omega) + \epsilon(\omega - \Delta)]l_i + \epsilon(\omega + \Delta)l_0\} \quad [13]$$

$\bar{R}$ and $\bar{I}$ are R and I per unit concentration, $\epsilon(\omega)$ is the *decadic* extinction coefficient at frequency ω, and l_i and l_0 are the distances into and out of the crossing point from the cell surfaces. Far from the maximum of the electronic transition γ becomes zero and $c_{opt} = 2c_0$. In all cases the signal drops off very rapidly for $c > c_{opt}$.

A simple evaluation of the optimum excitation wavelength for a real molecular solution is more complicated because of the difficulty of evaluating Eq. [7] for a broad electronic resonance. For the isolated electronic resonance (Eq. [8]) the quantity $R^2 + I^2$ is maximal when $D = \omega_e - \omega$ is the solution of the expression $D(D - \Delta) + \Gamma_e^2 = 0$. At this value of D, $R = 0$ and the imaginary component proportional to $2BI\Gamma_r$ must be included.

EXPERIMENTAL RESULTS

Fig. 1 shows the CARS spectrum of an aqueous solution of sodium benzoate in the region near $\Delta = 1000$ cm^{-1}. The spontaneous Raman spectrum shows peaks at 1005 cm^{-1} and 1027 cm^{-1}, with relative intensities of about 4 to 1. In the lower curve (0.3 M) the CARS signal is comparable to the background susceptibility. The dispersion-like cross term involving the product of the background susceptibility and the Raman susceptibility is clearly evident.

Fig. 2 shows a comparison of the CARS and spontaneous Raman spectra of diphenyloctatetraene in benzene at a concentration of 1.4×10^{-3} M in the 1100–1200 cm^{-1} region. The benzene peak at 992 cm^{-1} is also shown for comparison. In the Raman spectrum the peak at 1140 cm^{-1} has a cross section per molecule which is about 700 times that of the benzene 992 cm^{-1} mode. From the CARS spectrum a ratio of cross sections of about 3000 is obtained. This value is higher than the Raman value because it represents the ratio of the geometric mean of the cross sections at ω (4800 Å) and $\omega + \Delta$ (4550 Å) rather than the ratio of the cross sections at 4880 Å as in the Raman case. The background level in the spontaneous Raman spectrum in Fig. 2 is due to fluorescence.

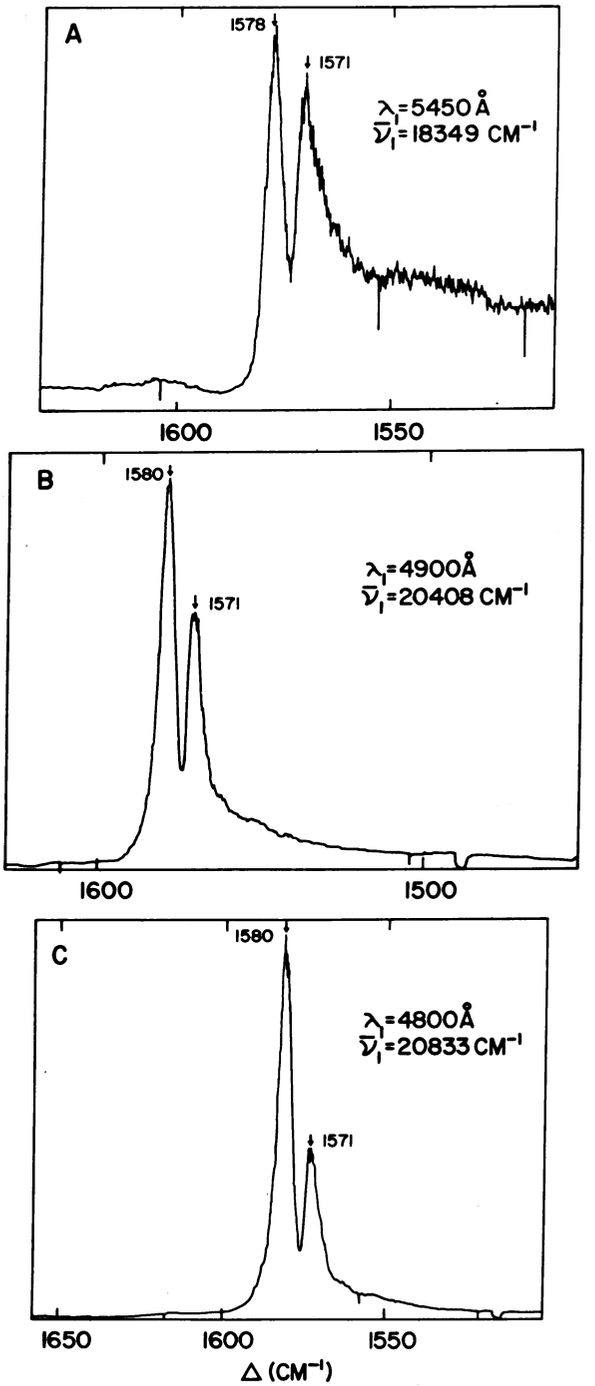

FIG. 3. The CARS spectrum of diphenyloctatetraene in benzene (1.4×10^{-3} M) in the 1500–1600 cm^{-1} region. The pump wavelength is (A) 5450 Å, (B) 4900 Å, and (C) 4800 Å. The small notches toward the right in (B) and (C) are zero level checks. For (C), $c_{opt} = 2c_0 = 1.6 \times 10^{-3}$ M (Eq. [13]).

Fig. 3 shows the CARS spectrum for three different pump

wavelengths of diphenyloctatetraene in benzene (1.4×10^{-3} M) in the 1500–1600 cm^{-1} region where there are two strong Raman lines (7). The first peak of the strong electronic absorption of the solute is at 4040 Å (24750 cm^{-1}) so that each of these cases correspond to "preresonance" enhancement. For $\lambda_1 = 5450$ Å the Raman contribution to the third order susceptibility, $\chi_r^{(3)}$, at this concentration is sufficiently small that the cross term with the solvent background makes the resonance highly asymmetric. For $\lambda_1 = 4900$ Å (Fig. 3B) or 4800 Å (Fig. 3C), $\chi_r^{(3)}$ is significantly increased, particularly for the 1580 cm^{-1} mode. The differential enhancement of the 1580 cm^{-1} mode compared to the 1571 cm^{-1} mode is of interest in polyene electronic spectroscopy in view of the fact that of these two modes, only the 1571 cm^{-1} mode appears in the high resolution fluorescence spectrum (7).

It is important to note that resonance enhancement of the CARS spectrum for this solution does not result in a proportional increase in the background susceptibility.

The intensity of the observed CARS peaks (above the background level) has been measured relative to features due to the benzene solvent. The use of this relative intensity ratio compensates for differences in the optimization of each experiment, laser power differences, and sample absorption. The observed intensity increase for the 1580 cm^{-1} mode on going from 5450 Å to 4800 Å is a factor of 6. This ratio may be estimated using Eq. [7]. In order to perform this calculation it is assumed that there are three equal intensity vibronic resonances at the three observed maxima, and that Γ_b, which is 100–300 cm^{-1}, can be ignored compared to the frequency differences which are at least 2300 cm^{-1}. Both terms are retained in each sum. The calculated intensity ratio is 5.7, in excellent agreement with experiment.

Coherent Stokes Raman scattering spectra have also been obtained by measurement of the signal generated at $\omega - 2\Delta$ (4) which show asymmetric features similar to Fig. 3A.

CONCLUSIONS AND DISCUSSION

The basic conclusion of this work is that resonance enhancement of CARS spectra is a feasible technique for extending the range of application of CARS to include dilute solutions. The problem of sample fluorescence is eliminated and the use of low average power should reduce sample damage significantly.

Acknowledgment is made to the donors of The Petroleum Research Fund, administered by the American Chemical Society, for partial support of this research through Grant no. PRF 8485-AC6 to B.H. The experiments described in this work were performed at Molectron Corporation, 177 N. Wolfe Road, Sunnyvale, Calif. 94086. The generosity of Molectron Corporation is gratefully acknowledged. This work has benefited greatly by conversations with Prof. Hans C. Andersen of Stanford University. B.H. is a Camille and Henry Dreyfus Teacher Scholar and an Alfred P. Sloan Foundation Fellow.

1. Begley, R. F., Harvey, A. B. & Byer, R. L. (1974) *Appl. Phys. Lett.* **25**, 387–390.
2. Begley, R. F., Harvey, A. B., Byer, R. L. & Hudson, B. S. (1974) *J. Chem. Phys.* **61**, 2466–2467.
3. Begley, R. F., Harvey, A. B., Byer, R. L. & Hudson, B. S. (1974) *Am. Lab.* **6**, 11–21.
4. Chabay, I., Klauminzer, G. K. & Hudson, B. S. (1976) *Appl. Phys. Lett.* **28**, 27–29.
5. Maker, P. D. & Terhune, R. W. (1965) *Phys. Rev.* **137**, A801–A818.
6. Terhune, R. W. & Maker, P. D. (1968) in *Lasers II*, ed. Levine, A. K. (Marcel Dekker, Inc., New York), pp. 295–372.
7. Hudson, B. S. & Kohler, B. E. (1973) *J. Chem. Phys.* **59**, 4984–5002.
8. Behringer, H. A. (1967) in *Raman Spectroscopy*, ed. Szymanski, H. A. (Plenum, New York), Vol. 1, pp. 168–223.
9. Schmid, E. D. & Brosa, B. (1973) *J. Chem. Phys.* **58**, 3871–3877.
10. Behringer, J. & Brandmuller, J. (1959) *Ann. Phys.* **4**, 234–242.
11. Ivanova, T. M., Yanovskaya, L. A. & Shorygin, P. P. (1965) *Opt. Spektrosk.* **18**, 206–211. [(1965) *Opt. Spectrosc.* **18**, 115–118.].
12. Birks, J. B. & Dyson, D. J. (1963) *Proc. R. Soc. London, Ser. A* **275**, 135–148.
13. Levenson, M. D. & Bloembergen, N. (1974) *Phys. Rev. B* **10**, 4447–4463.
14. Levenson, M. D. & Bloembergen, N. (1974) *J. Chem. Phys.* **60**, 1323–1327.